MODELLING MATERIAL PROPERTIES OF LEAD-FREE SOLDER ALLOYS

Zhanli Guo*, Nigel Saunders, Peter Miodownik, Jean-Philippe Schillé

Sente Software Ltd., Surrey Technology Centre, The Surrey Research Park, Guildford, Surrey, U.K.

* z.guo@sentesoftware.co.uk

Abstract

A full set of physical and thermophysical properties for lead-free solder (LFS) alloys have been calculated, which include liquidus/solidus temperatures, fraction solid, density, coefficient of thermal expansion, thermal conductivity, Young's modulus, viscosity and liquid surface tension, all as a function of composition and temperature (extending into the liquid state). The results have been extensively validated against data available in the literature. A detailed comparison of the properties of two LFS alloys Sn-20In-2.8Ag and Sn-5.5Zn-4.5In-3.5Bi with Sn-37Pb has been made to show the utility and need for calculations that cover a wide range of properties, including the need to consider the effect of non-equilibrium cooling. The modelling of many of these properties follows well established procedures previously used in JMatPro software for a range of structural alloys. This paper describes an additional procedure for the calculation of the liquid surface tension for multi-component systems, based on the Butler equation. Future software developments are reviewed including the addition of mechanical properties, but the present calculations can already make a useful contribution to the selection of appropriate new LFS alloys.

Keywords

Material properties, modelling, alloy design, thermodynamics, lead-free solder alloys

Introduction

To meet the requirements arising from environmental and health issues concerning the toxicity of lead, lead-free solder (LFS) alloys have been developed during the past decade to replace conventional Pb-Sn alloys. Studies on LFS materials were particularly accelerated in the last years due to the introduction of RoHS (*Restriction of Hazardous Substances*) Directive on 1 July 2006, i.e. all electrical and electronic products in the EU market must now pass RoHS compliance. Although many industries serving the information communications technology and consumer electronics have claimed their production has been completely redesigned to accommodate the newly developed LFS alloys, the long term effect of such a switch remains to be seen. It has become clear though that the cost and increased risk to industry is significantly greater that initially thought, and to close the remaining knowledge gaps could take several more years of investment and investigation. There is therefore still strong interest in developing new LFS alloys for improved performance, reliability and to reduce toxicity.

This has created a need for fundamental data that accurately describe the behaviour of these alloys in solder joints and which can also be used to develop appropriate reliability models. Although tremendous efforts have been made in this direction, there is still a definite lack of material data for LFS alloys. Most of the available references focus on data collected via experimental routes that are costly and time-consuming. Moreover, the fact that a large number of experiments are required to generate sufficient data to cover the multitude of proposed alloy types/compositions and conditions means experimentation is not always an option. Existing computer modelling work is normally based on finite-element analysis, dealing with real production and reliability issues. Although material properties are critical inputs for such types

of modelling, little work has been done on computer modelling the whole range of materials properties as a function of phase distributions calculated thermodynamically in real time.

As part of the process of developing new LFS alloys, thermodynamic calculations have been extensively used [1-5], and a number of thermodynamic databases have been developed specifically for this purpose [1,2]. However, the limitations of a purely thermodynamic approach are well known, in that it does not provide direct information for general material properties, such as physical, thermophysical and mechanical properties, which are the key to the application of any new solders. Such material properties are also critical inputs for the manufacturing and reliability modelling of soldered components or systems using finite element or finite difference simulation tools.

The calculation of material properties has been made possible in recent years following the development of JMatPro computer software [6]. To date, the application of this software has been mainly in the area of structural metallic alloys [7-10]. However, many of the requirements for material properties in solders are identical and the scientific basis for modelling solders is very similar. In particular, much of the development work for JMatPro is aimed at providing reliable material properties at temperatures approaching the melting point (T_m), which is a basic requirement for solder alloys where even the room temperature (T_0) properties of Sn-based solder alloys correspond to values of (T_0/T_m) of the order of 0.6.

The present paper reports recent progress made in extending JMatPro for use in Sn-based solder alloys. The status of thermodynamic calculations will be first briefly reviewed and discussed. The extension to calculation physical properties, such as thermal expansion coefficients, Young's/shear/bulk modulii, and surface tension of the liquid will then be described, with emphasis on their use for multi-component solder alloys. This is followed by some applications relating to selected alloys.

Thermodynamic Modelling

The use of CALPHAD (Calculations of Phase Diagrams) approach is well established [11,12] and the requirements to produce successful thermodynamic databases for use with multi-component alloys have been discussed in detail [12]. The current thermodynamic database includes the following elements:

$$Sn\text{-}Ag\text{-}Al\text{-}Au\text{-}Bi\text{-}Cu\text{-}In\text{-}Ni\text{-}Pb\text{-}Sb\text{-}Zn$$

Although the database was designed and tested for Sn-based alloys, the coverage of binary and ternary systems also allows it to be used at compositions where Sn may not be the major element. The database has been constructed by combining thermodynamic assessments of binary and ternary systems obtained from the open literature alongside extensive new work, including a complete coverage of binary assessments, and a wide range of ternary assessments covering all Sn-X-Y systems.

It should be noted that models and critical thermodynamic parameters from various published thermodynamic assessments in the literature may differ. For example, models for important phases may not be compatible and lattice stabilities for metastable crystal forms of the elements may not be the same. Therefore, as part of the database creation, self-consistent models for all phases and Gibbs energy functions for the pure elements were used. In a substantial number of cases, where otherwise good thermodynamic assessments were reported, re-modelling of key phases, such as those based on the B8 type phases, which include Cu_6Sn_5 and AuSn, was undertaken to provide internal self-consistency.

In recent years, substantial efforts were made to develop LFS alloys that are suitable substitutes for classic Pb-Sn eutectic solders. One basic requirement for the new alloys is to have the appropriate melting temperatures and freezing ranges (liquidus and solidus), in order to be compatible with existing equipment and components. The thermodynamic database can be used to predict these properties and also show the

effects of non-equilibrium solidification. The results from these predictions can be used to eliminate candidate solder alloys for which the calculation revealed unsuitable freezing temperature and range from further testing. This database has been tested extensively against experimental solders and Fig.1 shows a comparison plot for solidus and liquidus values for the solder alloys reported in the NIST solder alloy property database [13] and the Indium Corporation properties datasheet [14] (see Table 1 for details).

In certain cases, particularly those with higher levels of Cu and Ag additions, intermetallics may control the liquidus. However it is clear from the main source of data (Table 4.1 of Ref. 13) that the liquidus quoted is almost certainly for the temperature when Sn first forms and the calculated results are therefore given for this case. The most likely reason that the temperature for Sn formation appears in the tables of Ref. 13 is that this is a strong reaction, with a highly visible thermal signature. On the other hand the formation of minor amounts of intermetallic compound has a very small thermal signature, particularly when liquidus slopes are steep, as is the case for (Cu,Ag)-Sn compounds.

Modelling of Physical Properties

Thermophysical and physical properties are an important part of materials science, particularly at the present time when such data is a critical input for software programmes dealing with process modelling. A major achievement of the JMatPro software project has been the development of an extensive database for the calculation of such properties which can be linked to its thermodynamic calculation capability. For each individual phase in multi-component systems, properties, such as molar volume, thermal conductivity, Young's modulus, and Poisson's ratio, are calculated using simple pair-wise mixture models.

$$P = \sum_i x_i P_i^o + \sum_i \sum_{j>i} x_i x_j \sum_v \Omega_{ij}^v (x_i - x_j)^v \tag{1}$$

where, P is the property of the phase, P_i^0 is the property of the phase in the pure element, Ω_{ij}^v is a binary interaction parameter dependent on the value of v, x_i and x_j are the mole fractions of elements i and j in the phase. Both P_i^0 and Ω_{ij}^v are temperature dependent and it is possible to include ternary or higher order effects where appropriate.

Once the property of each individual phase is defined, the property of the final alloy can be calculated using appropriate mixture models [15,16]. Utilising well established relationships between certain properties (e.g. thermal and electrical conductivity), reduces the need for individual databases for each property. At present the properties that can be modelled include: volume, density, thermal expansion coefficient, Young's, bulk and shear modulii, Poisson's ratio, thermal conductivity and diffusivity, electrical conductivity and resistivity, viscosity and diffusivity of the liquid. The physical property models have been extensively tested and validated, particularly for solidification purposes [17].

Extensive work has been undertaken to build up and validate the requisite property databases for solder systems. Comparison of experimental and calculated densities for many solder alloys are shown in Fig.2 where the source of experimental data is again the NIST property database [13]. While calculations of room temperature properties such as density are relatively commonplace, all properties calculated by JMatPro are temperature dependent and include values for the liquid state. Analogous calculations for the coefficient of thermal expansion (CTE) and its temperature dependence are given in Fig.3 which shows a comparison of the calculated CTE of a solder alloy Sn-3.9Ag-0.6Cu (in wt%) with experiment [18]. Fig.4 shows a comparison of the calculated Young's Modulus with experiment. In Figs. 3 and 4, the symbols "#1" and "#2" denote two casts of the same alloy, whereas the labels "As cast" or "Aged" correspond to the condition in which the alloys were tested.

While the properties mentioned above are very important, it is also necessary to consider surface tension of solder alloys. For instance, surface tension is a critical input for the modelling of many steps in

manufacturing such as solder paste printing, solder bump solidification and solder joint shape. A theoretical treatment for binary alloys developed by Butler [19] has been used by numerous authors and has been well substantiated over the years [20-23]. However there has been much less work on devising an extension capable of handling multi-component alloys. The basic expression derived by Butler is as follows:

$$\sigma = \sigma_i^{[T]} + \frac{RT}{A_S}\ln(a_i^*/a_i) \tag{2}$$

where $\sigma_i^{[T]}$ is the surface tension of pure component i at temperature T, A_S is the molar surface area, a_i is the activity of component i (at temperature T) and a_i^* is the activity of component i in a monomolecular layer at the surface. A_S can be calculated via the molar volume $V_{m(i)}$ of the species via:

$$A_s = LN^{1/3}V_{m(i)}^{2/3} \tag{3}$$

where N is Avogadro's number and L is a constant reflecting the packing of atoms in the surface. Therefore, the three basic ingredients for any calculation of the surface tension of alloys are,
   (i) values for the surface tension (σ_i) of the pure elements,
   (ii) the molar volume ($V_{m(i)}$) as a function of composition,
   (iii) the activities (a_i^* and a_i) of the alloying components (i).

The activities have traditionally been expressed in terms of excess Gibbs energy parameters for the bulk liquid and corresponding values for a surface phase with a different number of nearest neighbours, which reflects the need to adjust bond angles and strength at the liquid-vapour interface. It has been generally assumed that $\ln(a_i^*)$ is linearly proportional to $\ln(a_i)$ with proportionality constant, β, related to the ratio of the number of nearest neighbours in the surface layer Z^* to the equivalent number Z in the bulk of the liquid.

Since values for M_v and a_i are already available from JMatPro, it is only necessary to evaluate the surface tension of the elements in the liquid state to calculate the surface tension for alloys. The results for binary alloys give a good match both with experiment [24,25] and in comparison with calculations from other groups [20] (Fig.5).

The reason why calculations for ternary and higher order alloys have only been considered relatively recently is because there is a marked increase in the number of required input parameters. Various workers have taken different approaches to this problem (see for example Pajarre et al. [26] and Tanaka and Iida [27]). For systems that are relatively ideal, the precise method adopted does not make much difference. However in the general case there can be appreciable deviations in activity from ideal and thermodynamic calculation is required for any approach to be predictive.

Experimental surface tension data for ternary or higher order systems is also rather sparse. Pajarre et al [26] only applied their treatment to Ag-Au-Cu and there are some earlier results for Cr-Fe-Ni [28]. Ternary data exists for solder systems such as Sn-Ag-Sb [3] and Sn-Ag-In [29], but these only contain relatively low levels of ternary additions because of the constraint of meeting melting point and freezing range requirements.

Our approach is also based on the Butler equation, but differs in detail on how it is extended to higher order systems [30]. The general accuracy achieved by JMatPro is illustrated in Fig.6 which shows that the accuracy for ternary alloys (Ag-Au-Cu [26], Cr-Fe-Ni [28], Sn-Ag-In [29], Sn-Ag-Sb [3]) is on par with that achieved for binary systems (Ag-Sn [21], Au-Cu [26], Au-Sn [31], Bi-Sn [20], Cu-Pb [24,25], Fe-Si [20], Pb-Sn [21]). One immediate advantage of such calculations is in interpreting the trend indicated by experimental results. In the absence of calculated values, it is very difficult to make a judgment about the

validity of some of the scattered results reported in the literature. The general accuracy attained also gives confidence in predicted results for systems for which no experimental results are available.

Selected Applications

A key area of research for lead-free solders has been to design a "drop-in" replacement for traditional Pb-Sn eutectic solders. One of the first key properties is that the liquidus and solidus temperatures should be close to the Pb-Sn eutectic temperature. In this respect it is instructive to look at two potential alloys Sn-5.5Zn-4.5In-3.5Bi alloy (Indalloy #231) and Sn-20In-2.8Ag (Indalloy #227) [14] (all compositions in wt%). These alloys have quoted freezing ranges between 174-186ºC and 175-187ºC respectively, in comparison to the eutectic melting of the Pb-37Sn alloy at 183ºC.

The first aspect to examine is the solidification behaviour of the two alloys as the solidification process of solders is an important factor in the design of LFS alloys. One limiting case for describing solidification behaviour is the lever rule (thermodynamic equilibrium), where it is assumed that complete diffusion occurs in the solid as well as in the liquid at each temperature during cooling. Therefore, all phases are in thermodynamic equilibrium at each temperature.

In reality, solidification invariably occurs under non-equilibrium conditions which can be modelled by the implementation of a simple kinetic model based on the so-called Scheil-Gulliver (SG) concept [32]. The SG model can be considered as a complementary limiting case to equilibrium solidification whereby it is assumed that solute diffusion in the solid phase is small enough to be considered negligible and that diffusion in the liquid is extremely fast, fast enough to assume that diffusion is complete.

Such solidification can be modelled quite straightforwardly using thermodynamic calculations [2,12], and the procedure has yielded excellent results for many other kinds of alloys [32]. The effect of non-equilibrium solidification has been modelled for the two LFS alloys and compared with equilibrium solidification in Fig.7. It can be seen that the effect of considering non-equilibrium conditions is that the solidification range is much expanded. In itself this makes the behaviour of the alloys quite different to the Pb-37Sn alloy, which transforms directly from liquid to solid at 183ºC. There is also a further consequence in that the final phase structure will be unstable and will potentially transform during use, even at room temperature.

We have also calculated and compared density, thermal conductivity, Young's modulus and the liquid surface tension for all three alloys, which are shown in Figures 8-11, with experimentally reported data included for reference. Here, we have assumed the solders are thermodynamically equilibriated.

Discussion

It can be seen from Fig.7 that the effect of considering non-equilibrium conditions is that the solidification range is much expanded. In itself this makes the behaviour of the alloys quite different to the Pb-37Sn alloy, which transforms directly from liquid to solid at 183ºC. There is also a further consequence in that the final phase structure will be unstable and will potentially transform during use, even at room temperature. As well as solidification being different, key material properties show significant differences, which can affect manufacturing processing as well as use in service.

The largest difference between the two potential replacement solders is with respect to density (Fig.8). This is not surprising, since they contain no lead. Predicted shrinkage when solidifying from 250ºC to RT is rather variable with values of -4.4%, -4.8% and –4.1% respectively calculated for Sn-37Pb, Sn-20In-2.8Ag and Sn-5.5Zn-4.5In-3.5Bi.

The modulus is rather similar for all three cases, but for the Sn-20In-2.8Ag there is a distinct increase in modulus compared to the Sn-37Pb alloy, which agrees with experiment observation [14]. For both the Sn-37Pb and Sn-20In-2.8Ag, calculated values are higher that reported by Ref. 14, but it is noted that experimentally modulus for solder alloys can show wide variation as shown in Figure 9 for Sn-37Pb [13,14].

In terms of calculated thermal conductivities, the Sn-20In-2.8Ag alloy lies very close to Sn-37Pb, while the value for Sn-5.5Zn-4.5In-3.5Bi is substantially higher (Fig.10). Finally, both the potential replacement solders are predicted to have a substantially higher liquid surface tension than Sn-37Pb [33], which will affect wettability and subsequent manufacturing processes (Fig.11).

It would appear that at their present level, the calculations can give very reasonable values in terms of magnitude and good results with respect to the observed trend on alloying. As far as predicting results for new alloys is concerned, the methodology outlined in the present paper can by-pass some of the problems due to the large scatter in the experimental results available in the literature for the current generation of alloys. The thermal and/or deformation history of the sample is rarely recorded, and the microstructural features of the specimens are not always available. The fact that room temperature is close to 60% of the melting temperature for most of the solder alloys means that the microstructure can be unstable even during laboratory experiments. In the circumstances, the variation in recorded results is probably better described as erratic rather than random. While this paper has largely concentrated on calculating changes in associated physical properties, it is clear that knowledge of the mechanical properties would also benefit the development of better solder alloys. JMatPro already has models for the calculation of high temperature mechanical properties in structural alloys over a wide range of values for (T/Tm) [34] which allows the flow stress to be calculated as a function of temperature and strain rate up to the melting point and into the mushy zone and liquid which is as important to the integrity of soldered joints as it is it to other casting applications [35]. Experience has shown that calculated material data allows existing FEM techniques to give more realistic results than can be achieved where the input data is assumed to be independent of composition or temperature.

Summary and Future Work

Work has been reported on the extension of the Materials Property Software, JMatPro, for application to solder alloys. Thermodynamic, thermophysical and physical properties of solder alloys have been calculated and results validated against experiment. Surface tension calculations have been made and applied to both binary and higher order alloys. Work is on-going concerning the addition of mechanical properties and the extension of the surface tension calculations to wettability, as this is a major ultimate requirement (see Appendix Table A for a full list of current and projected properties).

The models used in the present calculations consider solders as isotropic materials, but it is well understood that modulus can change with crystallographic orientation, and that the use of fluxes will affect the experimentally measured surface tension. Nonetheless, it should be emphasised that the existing software can already make useful predictions for the design of solders with specific target properties in mind, for example a combination of low shrinkage, low modulus and high thermal/electrical conductivity and to generate a figure of merit combining several properties. It can clearly also be used to eliminate inappropriate alloys. Today's electronics industry is a severely competitive place, so any technique that helps to rapidly evaluate alternative alloy compositions and highlight potential ways of reducing cost could offer companies considerable advantages.

Acknowledgments

Appendix

In February 2001, a workshop on Modelling and Data Needs for Lead-Free Solders was held in New Orleans, L.A. The report summary of this workshop [36] described the scientific needs by the microelectronics community, and has been serving as a roadmap for research in the reliability of lead-free solders. The information on the priority level for various material properties given in Table A was taken from this report for Sn-3.9Ag-0.6Cu, Sn-0.7Cu, Sn-3.5Ag and Sn-37Pb (all in wt%) solder alloys. The present capabilities of JMatPro on property modelling is shown in Table I as well, together with JMatPro's planned development in near future.

References

1. U.R. Kattner, *JOM*, December, (2002), 45-51.
2. X.J. Liu I. Ohnuma, C.P. Wang, M. Jiang, R. Kainuma, K. Ishida, M. Ode, T. Koyama, H. Onodera and T. Suzuki, *J. Electron. Mater.*, 32, (2003), 1265-1272.
3. Z. Moser, W. Gasior, J. Pstrus, S. Ishihara, X.J. Liu and I. Ohnuma, *Mater. Trans.*, 45, (2004), 652-660.
4. N. Moelans, K.C. Hari Kumar and P. Wollants, *J. Alloys & Compounds*, 360, (2003), 98-106.
5. S.W. Yoon, J.R. Soh, H.M. Lee and B.J. Lee, *Acta Mater.*, 45, (1997), 951-960.
6. N. Saunders, Z. Guo, X. Li, A.P. Miodownik and J.P. Schillé, *JOM*, December, (2003), 60-65.
7. N. Saunders, *Aluminium Alloys, Their Physical and Mechanical Properties*, eds. J.F. Nie et al. (Melbourne, Australia: Inst. Mater. Eng. Australasia), 96.
8. X. Li, A.P. Miodownik and N. Saunders, *Mater. Sci. Tech.*, 18, (2002), 861.
9. N. Saunders, Z. Guo, X. Li, A.P. Miodownik and J.P. Schillé, Superalloys 2004 (10th International Symposium on Superalloys, 19-23 September, 2004, Champion, Pennsylvania), eds. K. Green et al. (Warrendale, PA: TMS, 2004), 849-858.
10. N. Saunders, X. Li, A.P. Miodownik and J.-Ph.Schillé, Ti-2003 Science and Technology, eds. G. Luetering and J. Albrecht, (Weinheim, Germany: Wiley-VCH, 2004), 1397-1404.
11. L. Kaufman and H. Bernstein, *Computer Calculations of Phase Diagrams*, (New York: Academic Press, 1970)
12. N. Saunders and A.P. Miodownik, *CALPHAD – Calculation of Phase Diagrams*, *Pergamon Materials Series vol.1*, ed. R.W. Cahn, (Oxford: Elsevier Science, 1998).
13. T. Siewert, S. Liu, D.R. Smith, and J.C. Madeni, *Properties of Lead-Free Solders, Release 4.0*, (NIST and Colorado School of Mines, 2002) http://www.boulder.nist.gov/div853/lead%20free/solders.html
14. Indium Corporation of America, Europe and Asia, http://www.indium.com/products/alloychart.php
15. Z. Fan, P. Tsakiropoulos and A.P. Miodownik, *J. Mat. Sci.*, 29 (1994) 141.
16. Z. Fan, *Phil. Mag. A*, 73 (1996), 1663.
17. N. Saunders, X. Li, A.P. Miodownik and J.P. Schillé, *Modelling of Casting, Welding and Advanced Solidification Processes X*, eds. D. Stefanescu, J.A. Warren, M.R. Jolly and M.J.M. Krane (Warrendale, PA: TMS, 2003), 669-676.
18. P.T. Vianco, Sandia Laboratories (2001) as given in ref. [**Error! Bookmark not defined.**].
19. J.A.V. Butler, *Proc. Roy. Soc A*, 135, (1932), 348.
20. T. Tanaka, K. Hack and S.Hara, *MRS Bull.*, April, (1999), 45.
21. J.H. Lee and D.N. Lee, *J. Electron. Mater.*, 30, (2001), 1112.
22. W. Gasior, Z. Moser and A. Debski., *Arch. Metall. & Mat.*, 49, (2004), 575.
23. R. Picha, J. Vrestal and A. Kroupa, *CALPHAD,* 28, (2004), 141.
24. G. Metzger, Z. Phys. Chem, 211, (1959), 1.

25. J.C. Joud, N. Eustathopoulos, A. Bricard and P. Desre, *J. Chim. Phys.*, 70, (1973), 1290.
26. R. Pajarre, P. Koukkari, T. Tanaka and J. Lee, *CALPHAD*, 30, (2006), 196.
27. T. Tanaka and T. Iida, *Steel Research*, 65, (1994), 21.
28. K. Mori, M. Kishimoto, T. Shimose and Y. Kawai, *J. Jap. Inst. Metals*., 39, (1975), 1301.
29. X.J. Liu,Y. Inohana, I. Ohnuma, R. Kainuma, K. Ishida, Z. Moser, W. Gasior and J. Pstrus, *J. Electron. Mater.*, 31, (2002), 1139.
30. A.P. Miodownik *in preparation*
31. R. Novakovic, E. Ricci, F. Gnecco, D. Giuranno and G. Borzone, *Surface Science*, 599, (2005), 230-247.
32. N. Saunders, in *Solidification Processing 1997*, eds. J. Beech and H. Jones, University of Sheffield, Sheffield, 1997, 362-366.
33. http://www.interfluxusa.com/Technical/Sixsigma.htm
34. N. Saunders, Z. Guo, X. Li, A.P. Miodownik and J.P. Schillé, *JOM*, 55 (12), (2003), 60-65
35. Z. Guo, N. Saunders, A.P. Miodownik and J.P. Schillé, *Materials Science and Engineering* A413-414, (2005), 465-469
36. http://www.nemi.org/cms/newsroom/Presentations/ lf_workshop_report.html

Table 1. Composition range and number of alloys used in Fig.1

Element	max level (wt%)
Sn	Balance
Ag	7
Au	10
Bi	67
Cu	4
In	66
Pb	97
Sb	10
Zn	9
Number of alloys	236

Appendix Table A, Industrial list of priorities of materials properties

CTE (liquid and solid state)	1	*
Volume Change on freezing (liquid and solid state)	1	*
Specific Heat	3	*
Latent Heat	3	*
Thermal Diffusivity	3	*
Thermal Conductivity	3	*
Electrical Conductivity/Resistivity	3	*
Surface Tension at temp of solder	2	*
Wettability	2	**
Shear Strength (strain rates (SRs) from 10^{-1} to 10^{-6} s^{-1})	1	**
Ring in Plug (SRs from 10^{-1} to 10^{-6} s^{-1})	3	
E (Young's modulus) at 25°C	1	*
E at 50, 100 and 125°C	1	*
Total Elongation (SRs from 10^{-1} to 10^{-6} s^{-1})	1	**
Uniform Elongation (SRs from 10^{-1} to 10^{-6} s^{-1})	1	
UTS at 25°C	1	**
Yield Strength (SRs from 10^{-1} to 10^{-6} s^{-1})	1	**
Hardness	3	**
Work Hardening Coefficient (SRs from 10^{-1} to 10^{-6} s^{-1})	1	**
Creep Resistance (SRs from 10^{-1} to 10^{-6} s^{-1})	1	**
Min. Creep Strain rate at Stress of 20MPa at R°	1	**
Min. Creep Strain rate at Stress of 20MPa at 125°C	1	**
Thermomechanical Fatigue resistance(SRs from 10^{-1} to 10^{-6} s^{-1})	1	
Isothermal Fatigue Data (SRs from 10^{-1} to 10^{-6} s^{-1})	1	
Thermal Fatigue Hysteresis behaviour(SRs from 10^{-1} to 10^{-6} s^{-1})	1	
Constitutive Behavior(SRs from 10^{-1} to 10^{-6} s^{-1})	1	**
Stress Rupture(SRs from 10^{-1} to 10^{-6} s^{-1})	3	**
Dynamic Acoustic Measurements	3	
Fracture Toughness at R° (SRs from 10^{-1} to 10^{-6} s^{-1})	3	

1 = high Priority, 2 = medium priority, 3 = low priority
* Existing features of JMatPro
** Features to be implemented in the near future
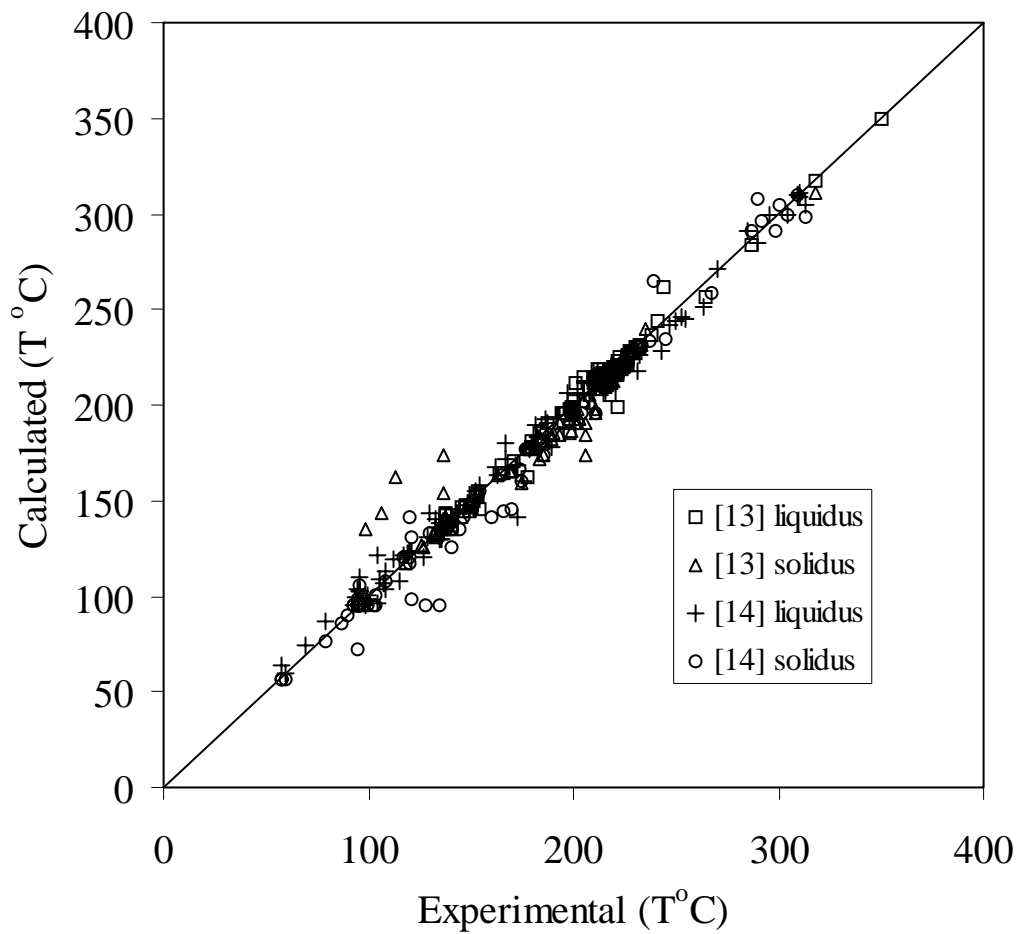
Fig. 1: Comparison between experimental [13,14] and calculated liquidus and solidus temperatures for various solder alloys
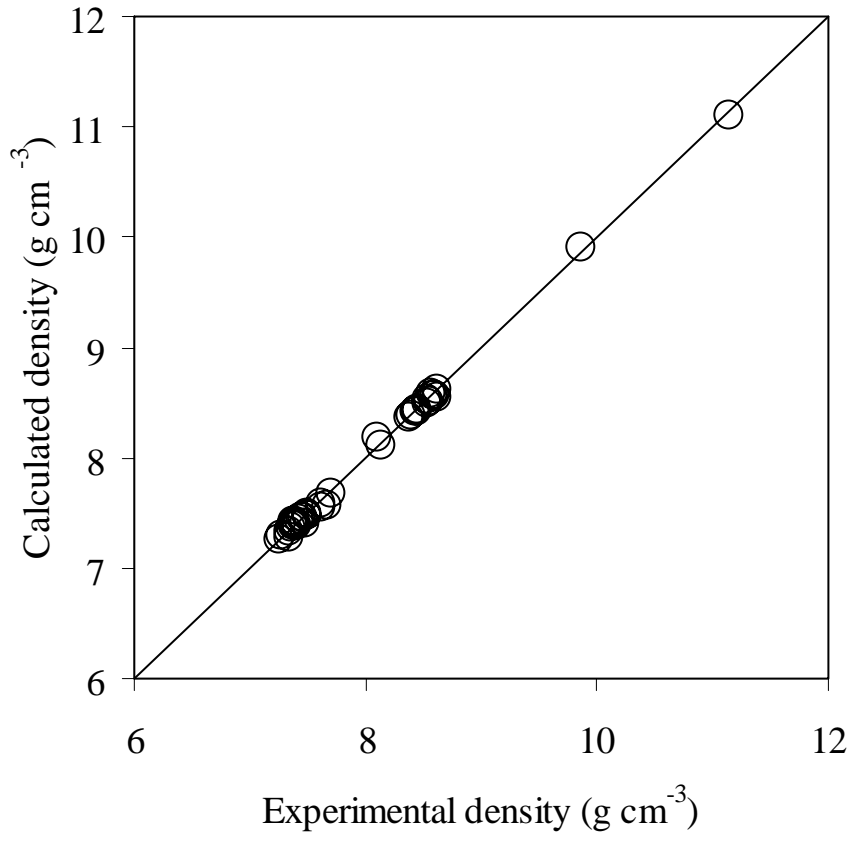
Fig. 2: Comparison between experimental [13] and
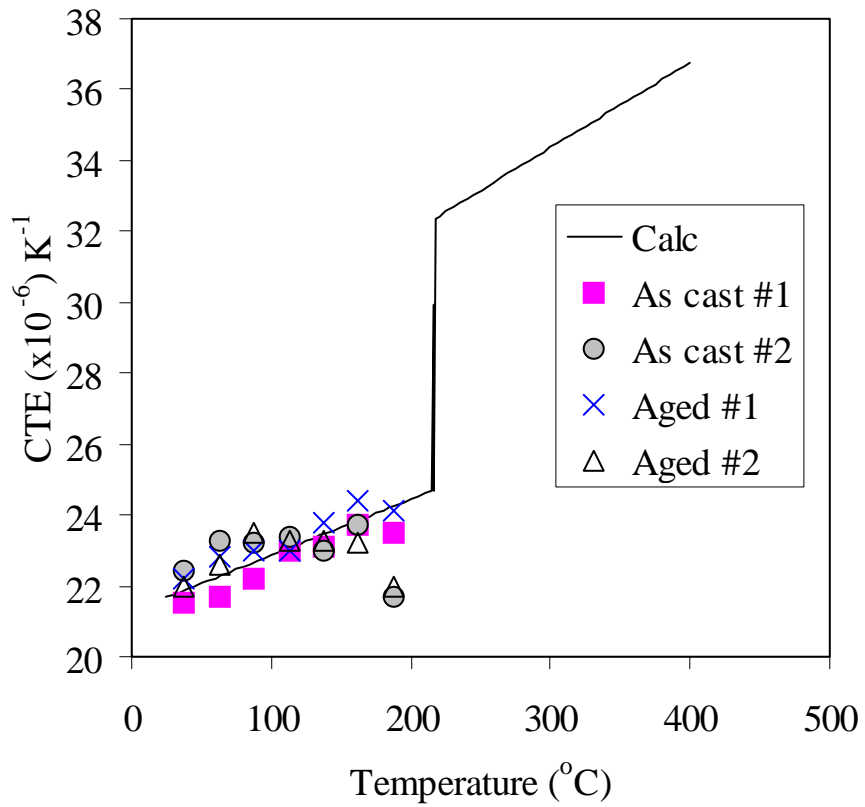calculated densities of various solder alloys

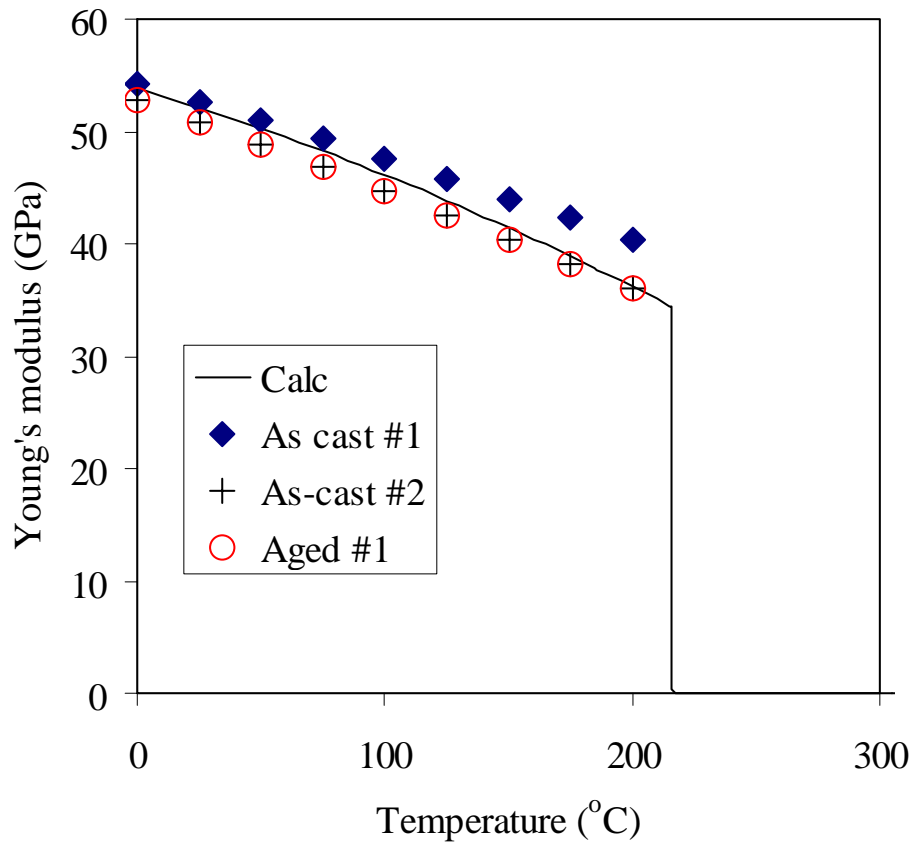Fig. 3: Comparison between experimental [18] and calculated CTE of Sn-3.9Ag-0.6Cu solder alloy

Fig. 4: Comparison between experimental [18] and calculated
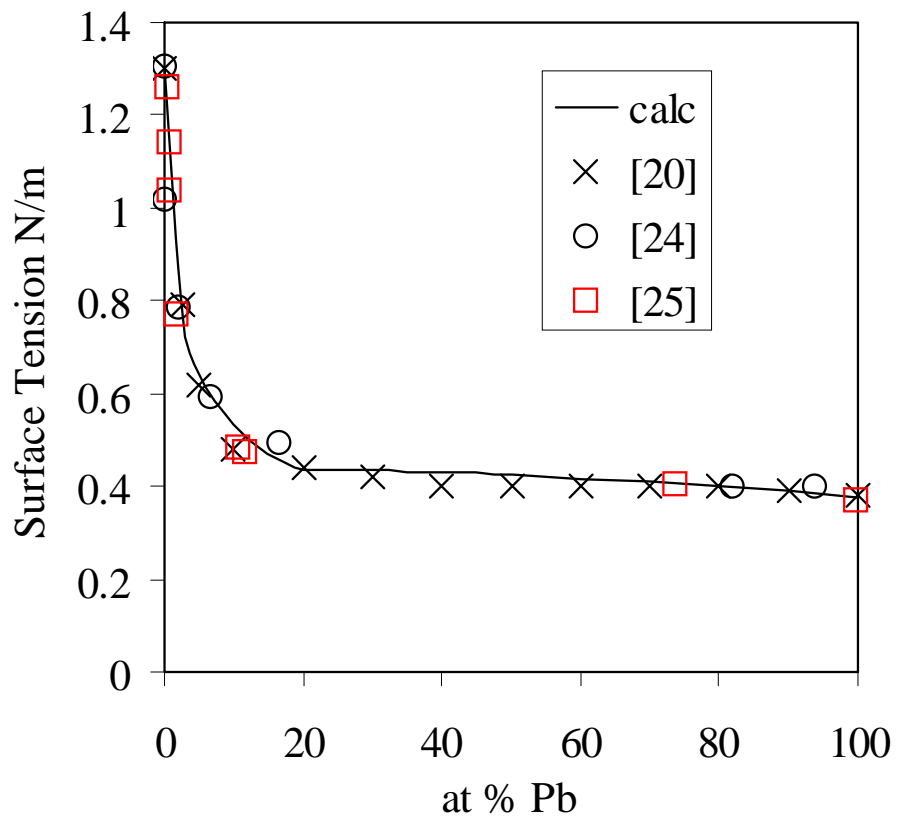Young's modulus of Sn-3.9Ag-0.6Cu solder alloy

Fig.5: Comparison between calculated, experimental [24,25] and previous calculation [20] of liquid surface tension in Cu-Pb alloys at 1100ºC.
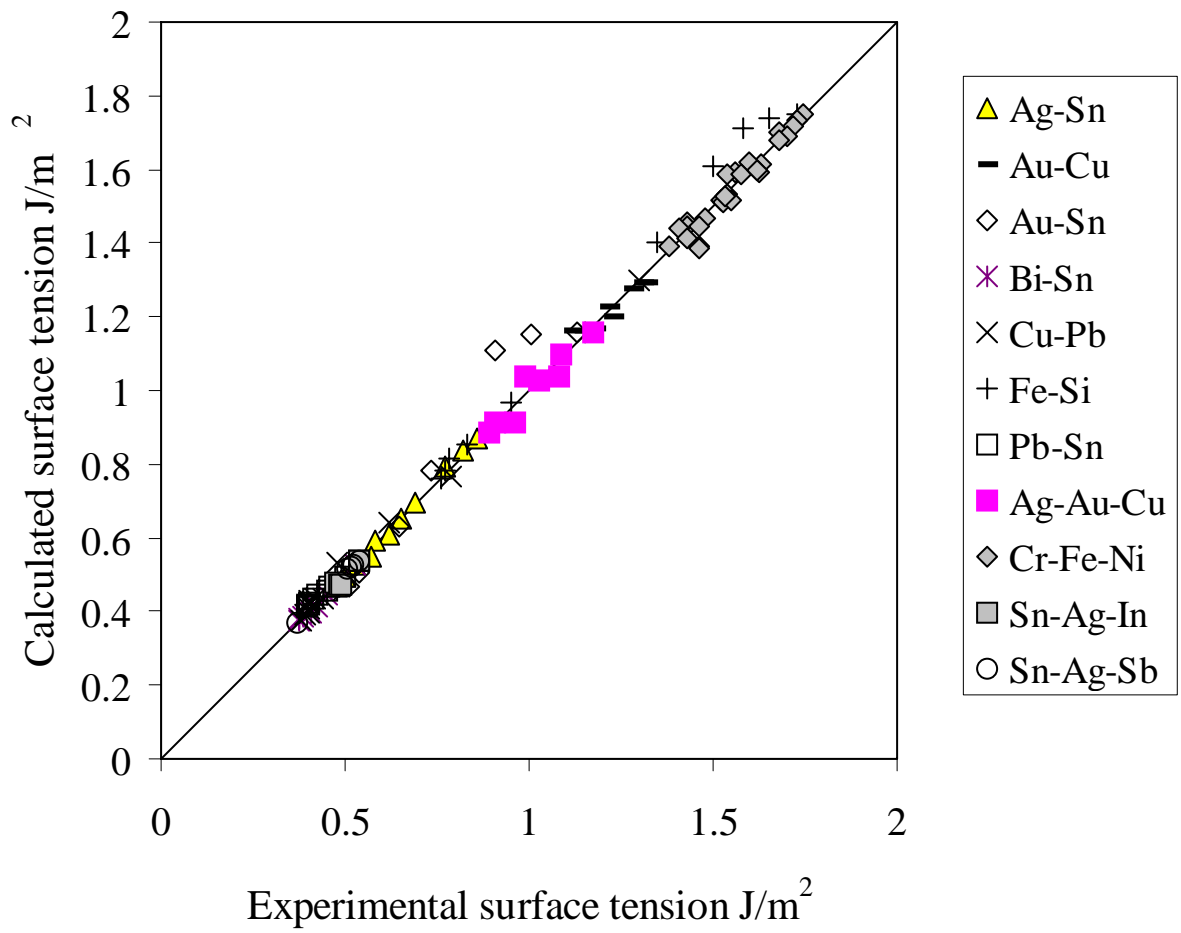
Fig.6: Comparison between experimental and calculated liquid surface tension for various binary and ternary alloys
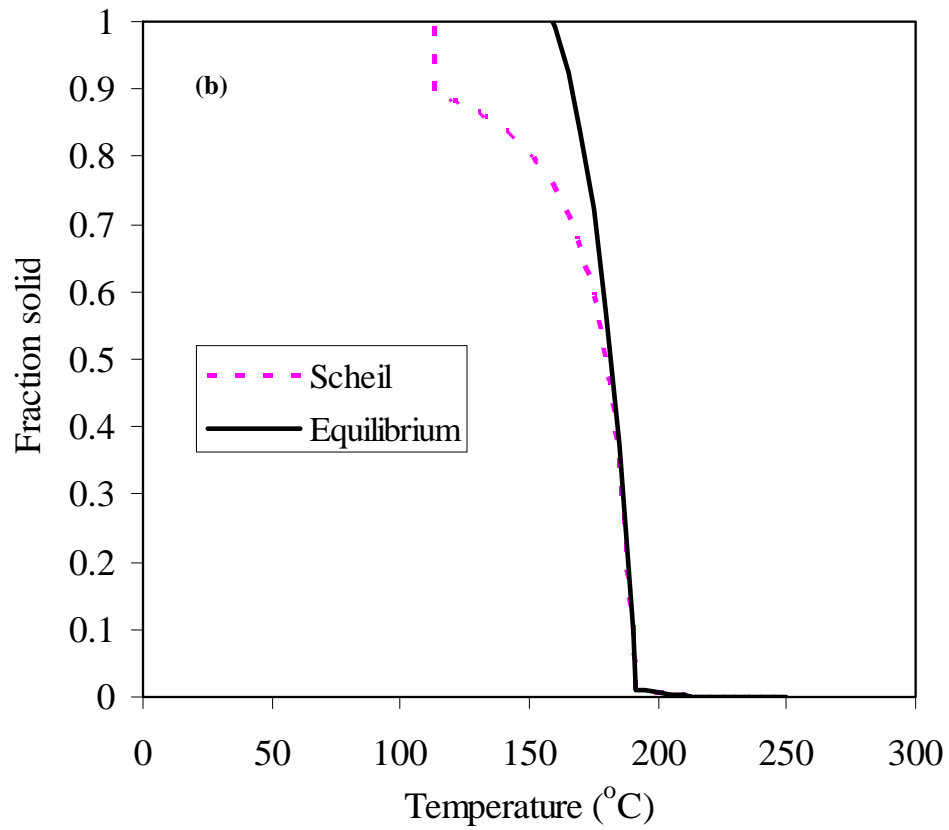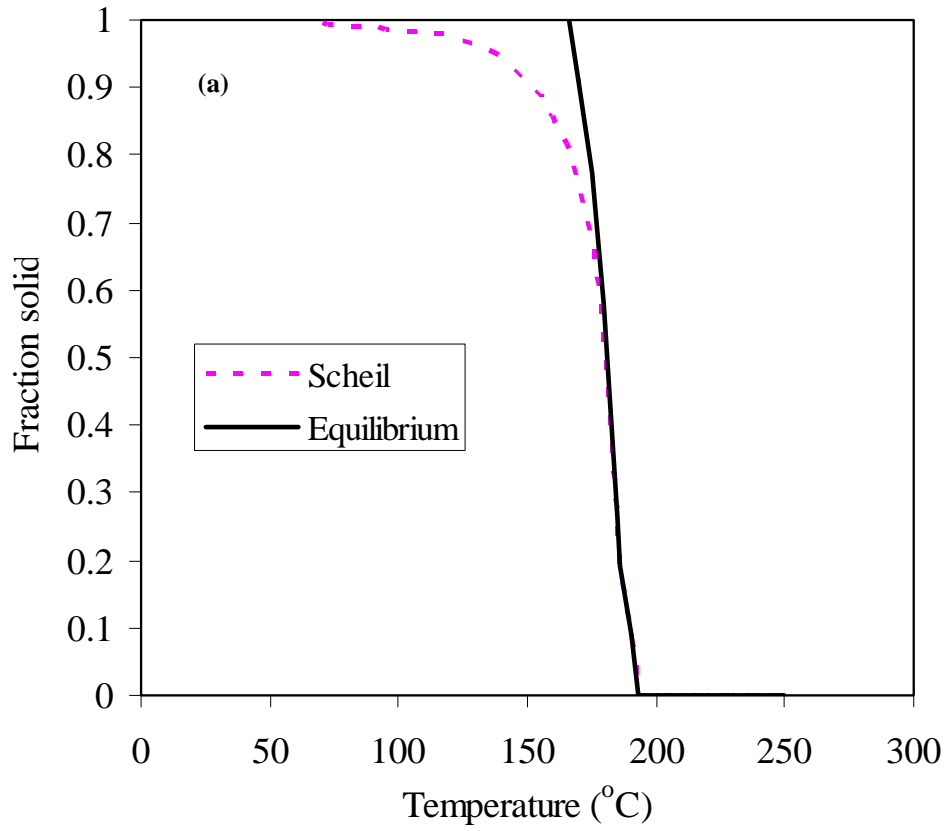
Fig.7: Comparison between equilibrium calculation and Scheil-Gulliver calculation for (a) Sn-5.5Zn-4.5In-3.5Bi, and (b) Sn-20In-2.8Ag solder alloys
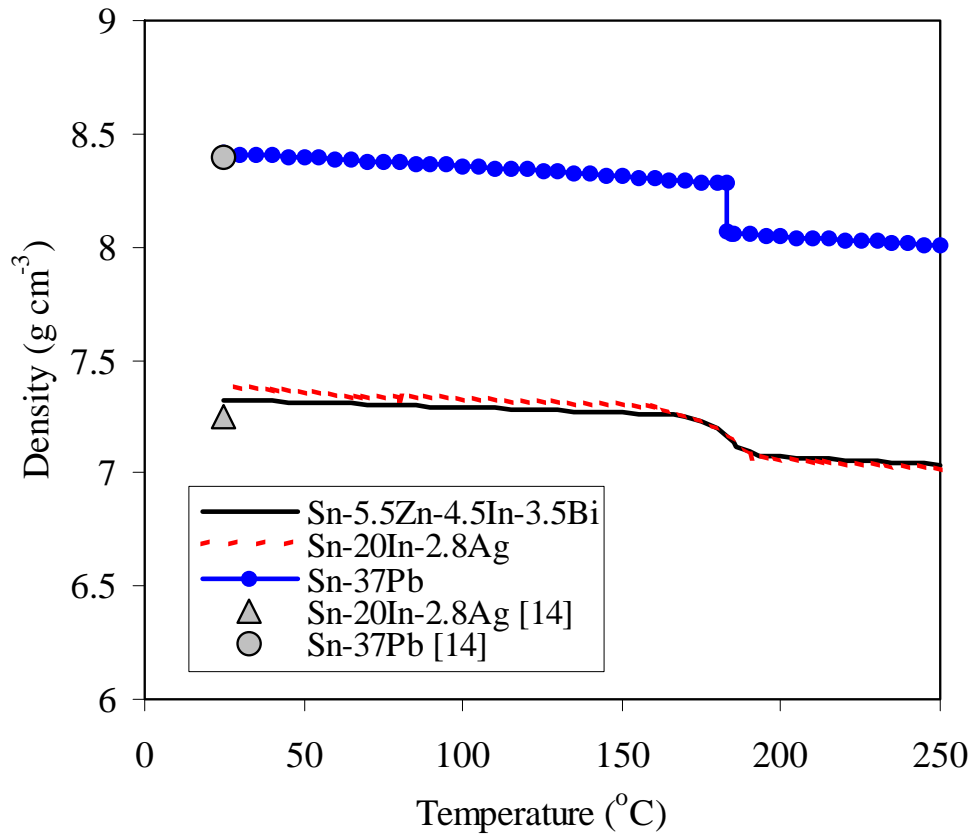
Fig.8: Calculated density change with temperature for Pb-37Sn, Sn-5.5Zn-4.5In-3.5Bi, and Sn-20In-2.8Ag solder alloys
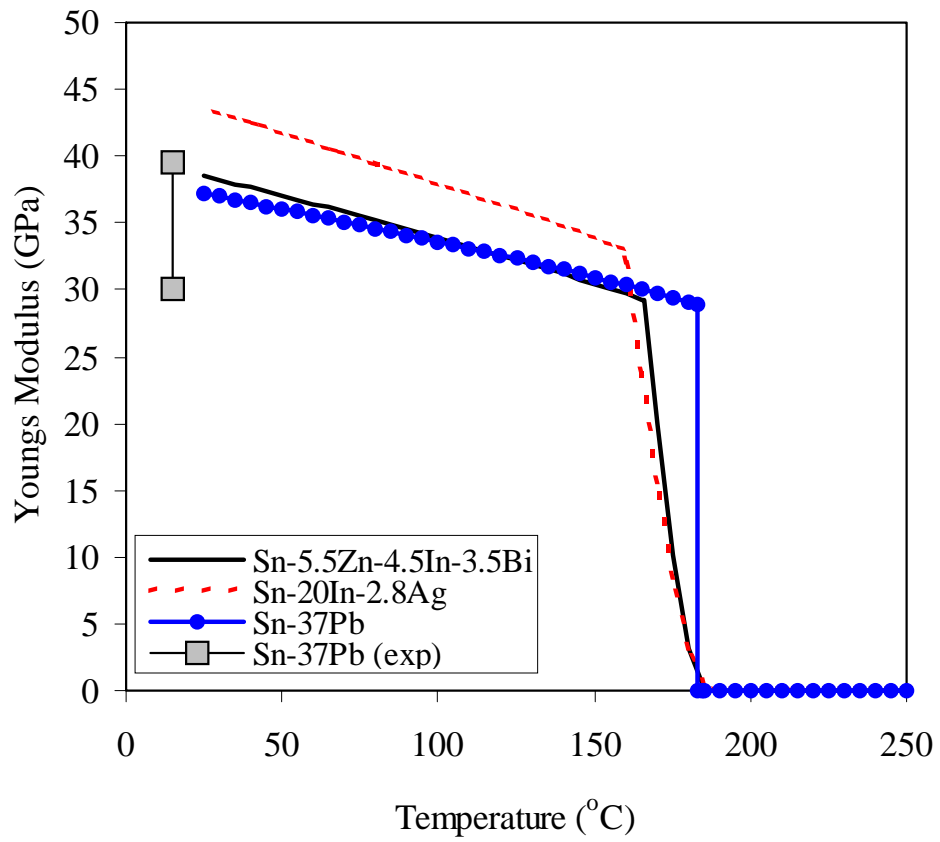
Fig.9: Young's modulus change with temperature for Pb-37Sn, Sn-5.5Zn-4.5In-3.5Bi, and Sn-20In-2.8Ag solder alloys
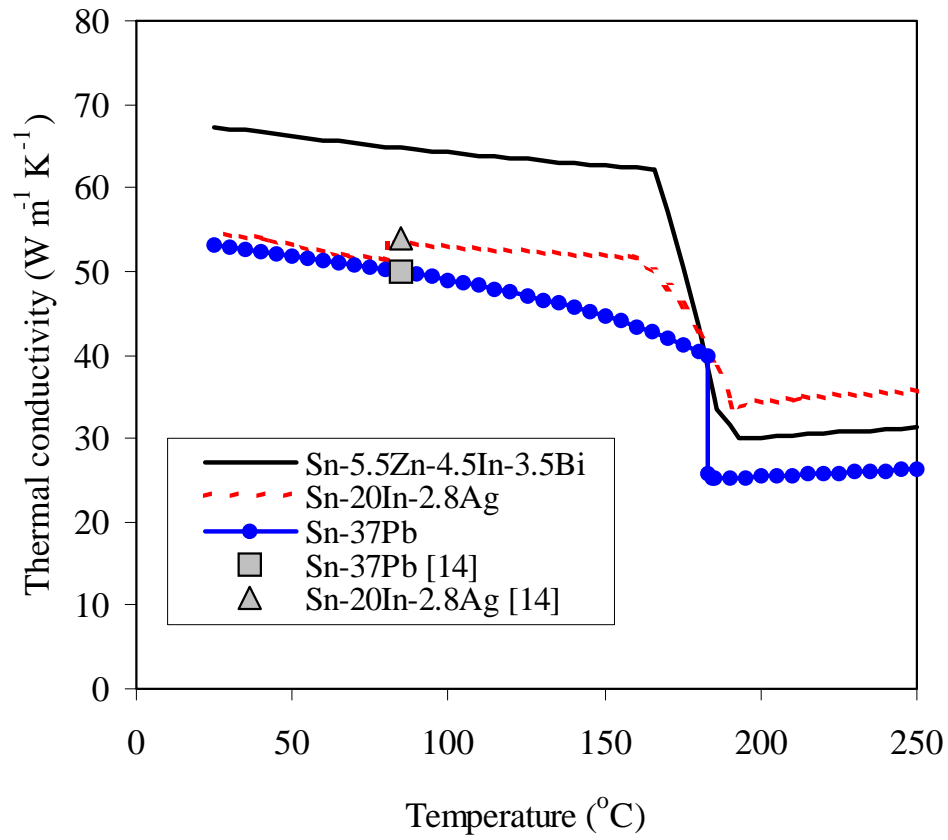
Fig.10: Thermal conductivity change with temperature for Pb-37Sn, Sn-5.5Zn-4.5In-3.5Bi, and Sn-20In-2.8Ag solder alloys
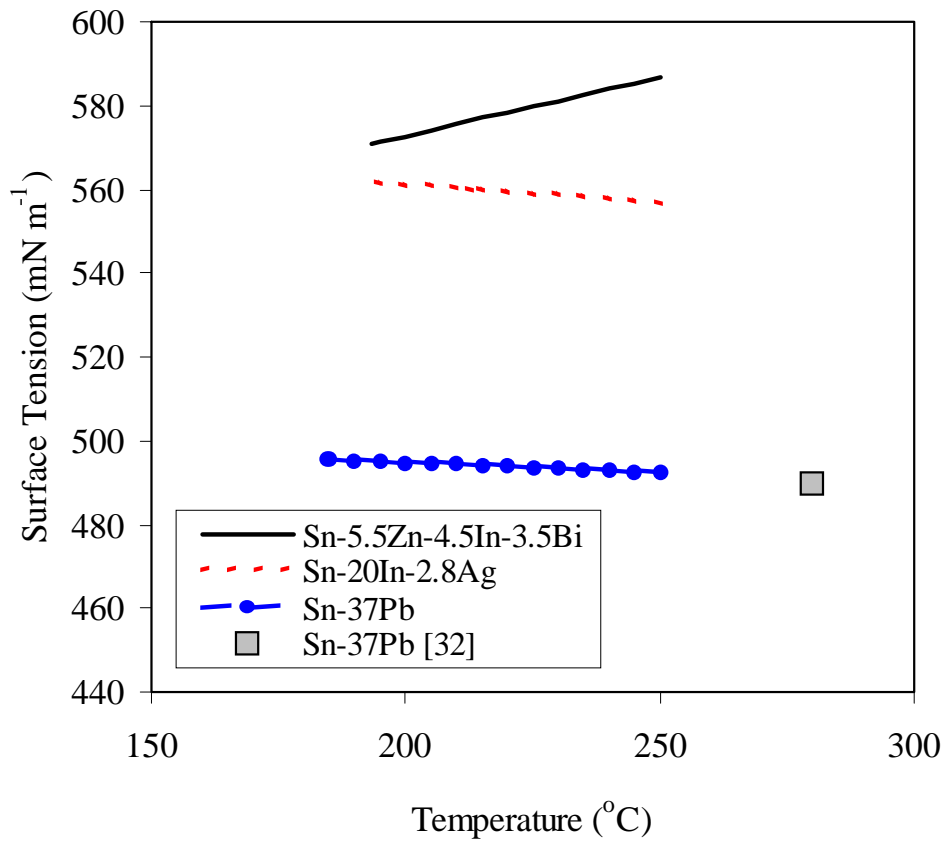
Fig.11: Surface tension change with temperature for Pb-37Sn, Sn-5.5Zn-4.5In-3.5Bi, and Sn-20In-2.8Ag